Erschienen in: 7th International Conference on Silicon Photovoltaics, SiliconPV 2017, 3-5 April 2017, Freiburg, Germany / Preu, Ralf (Hrsg.). - Amsterdam : Elsevier, 2017. - (Energy Procedia ; 124). - S. 113-119
https://dx.doi.org/10.1016/j.egypro.2017.09.325

Available online at www.sciencedirect.com

ScienceDirect

Energy Procedia 124 (2017) 113–119

Energy Procedia

www.elsevier.com/locate/procedia

7th International Conference on Silicon Photovoltaics, SiliconPV 2017

Extraction of individual components of series resistance using TCAD simulations meeting the requirements of 2- and 3-dimensional carrier flow of IBC solar cells

Gabriel Micard*, Daniel Sommer, Giso Hahn, Barbara Terheiden

University of Konstanz, Department of Physics, 78457 Konstanz, Germany

Abstract

The series resistance (R_S) of a solar cell, that influences fill factor and thus efficiency, is usually decomposed into individual components for development of optimization strategies. In this contribution we introduce a method to extract R_s of each part of the solar cell from TCAD simulation using free energy loss analysis. This method is particularly relevant for modern cell concepts where only TCAD simulation describes correctly high injection phenomena in lowly doped wafers, and where 2- or 3-dimensional carrier flow occurs (PERC, PERT, IBC) invalidating the classical analytical models for R_s description. We compare the lumped R_S value extracted from the FELA to the R_S extracted from the Multiple Light Intensity Method (MLIM) for IBC solar cells with various geometries and wafer doping levels, with and without a front surface field, and show that it is quite accurate even when high injection phenomena induce a slight underestimation of R_S.

Peer review by the scientific conference committee of SiliconPV 2017 under responsibility of PSE AG.

Keywords: Series resistance; IBC solar cells; TCAD simulation

1. Introduction

For Si solar cells, R_s is an important and intricate parameter that describes alone the Joule losses of the solar cell in the corresponding equivalent circuit. For optimization strategies in solar cell development, it is crucial to evaluate

* Corresponding author. Gabriel Micard Tel.: +49 7531 882132; fax: +49 7531 883895.
E-mail address: gabriel.micard@uni-konstanz.de

1876-6102
Peer review by the scientific conference committee of SiliconPV 2017 under responsibility of PSE AG.
10.1016/j.egypro.2017.09.325

and predict the contribution of each part of the solar cell to the total, or lumped, R_s of the solar cell which can be extracted from measurement or simulation [1].

The typical method for R_s analysis is to determine each single component by using a set of analytical formulae, add these different R_s contributions and compare the total value to the lumped R_s value evaluated from the experimental IV curve. However, modern solar cell concepts such as the interdigitated back contact (IBC) Si solar cell have local p^+ and n^+ contacts on one or both sides implying a 2- or 3-dimensional current transport in the wafer. In this case classical models for R_s calculation from geometry and layer resistivity are inaccurate or require the excess carrier density from a TCAD simulation [2,3] making simulation the only way to evaluate individual R_s components.

The usual simulation to evaluate R_s specifically [4-6] assumes a current of one carrier type moving by drift (monopolar transport [7]) in a medium with a given conductivity. However, in a lowly doped wafer which is in moderate to high injection as in case of many promising cell concepts [8], the conductivity is a function of illumination and of the biasing of the solar cell (conductivity modulation [3]) that could be correctly evaluated only through TCAD simulation.

The goal of this contribution is therefore to introduce a method based on the free energy loss analysis (FELA) developed by Brendel *et al*. [9] allowing the extraction of individual R_s contributions directly out of a technology computer assisted design (TCAD) bipolar simulation.

We validate the method by investigating a typical design of IBC solar cells featuring high injection in the bulk, 2-D carrier transport and a floating doped region (the front surface field FSF) which are all the main challenges one encounters in a modern solar cell to evaluate individual components of series resistance.

2. Modeling

2.1. Structure and simulation parameters

As shown in Fig. 1, the 2-D unit cell used to describe the IBC solar cell in TCAD Sentaurus extends from half the back surface field (BSF) contact to half the emitter contact assuming one metal finger per emitter stripe. We introduce a small intrinsic gap (some µm) between the highly doped emitter and BSF to avoid high parasitic saturation currents which has, however, no significant impact on the R_s value. We chose to show a typical cell with a total cell width of 1500 µm where the fraction of the rear surface area covered by emitter, α, is varied between 0.5 and 0.9. The cell thickness is kept constant at 180 µm, which is standard for slurry sawn Czochralski-Si wafers.

We used standard doping profiles for emitter, BSF and FSF (R_{FSF} = 130 Ω/sq, J_{oFSF} = 25 fAcm^{-2}, R_{emi} = 60 Ω/sq, J_{oemi} = 125 fAcm^{-2}, R_{BSF} = 50 Ω/sq, J_{oBSF} = 125 fAcm^{-2}) for which the attributed surface recombination velocity (SRV) lies between 1,000 – 32,000 cm/s, according to [13] matching J_o (saturation current density) values. The wafer is a high quality n-type Si (mid-gap Shockley-Read-Hall lifetimes τ_p = 10 ms) with a resistivity of 1 or 8 Ωcm. Contact openings are 80 µm (typical for relaxed alignment conditions of laser contact opening and screen printing) with contact resistance ($R_{c,p}$ = 45 mΩcm², $R_{c,n}$ = 5 mΩcm²) assuming an SRV equal to the thermal velocity. State-of-the-art physical models and parametrizations [10] are used for all simulations. The described parameter set is compatible to state-of-the-art industrial-type IBC solar cells [8,11] with efficiencies well above 20%.

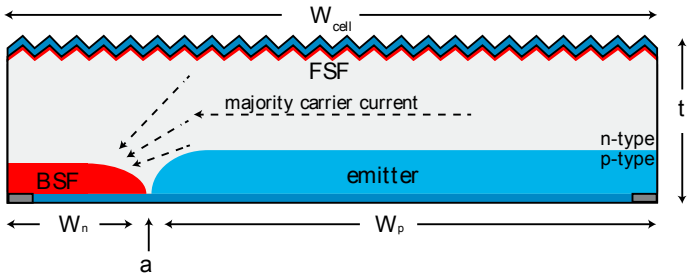

Fig. 1. Schematic structure of a 2-D unit cell for an IBC solar cell

2.2. Theory and justification

In a solar cell, the area normalized free energy dissipation rate occurring during the transport of electrons and holes, the Joule loss for electrons and holes by definition, in the i^{th} region of the solar cell can be defined using FELA [9] as:

$$\Phi_{e,h;i} = A^{-1} \int_{V_i} \left| \nabla \psi_{f;e,h} \right|^2 \cdot \sigma_{e,h} dV \quad (1)$$

with V_i the volume of region i, A the area of the solar cell, $\psi_{e,h}$ and $\sigma_{e,h}$ the quasi-Fermi potential and conductivity associated to electrons and holes. While the original formulation of Eq. 1 used current densities (Eq. 18 and 19 in [9]), we observed that the present formulation leads to the lowest discrepancy in the numerical evaluation of the net output energy flux between the FELA and the IV curve at the maximum power point.

The link between the Joule losses dissipated in R_s and the above defined Joule loss for electrons and holes is, however, not as clearly defined as for a monopolar theory (see [5,6]) mainly because additionally to drift, that is involved alone to describe the carrier transport in a resistance (Ohm's law), diffusion plays also an important role in the carrier transport in semiconductor device.

To evaluate the relative importance of drift versus diffusion, the Peclet number (Pe) is a useful concept stemming from hydrology. This dimensionless number expresses the ratio of the travel time due to drift and travel time due to diffusion and from its definition in hydrology (first form of Eq. 2, Eq. 2.6.8 in [12]), one can make use of the Einstein relations to bring it in the following relevant form for semiconductor devices.

$$Pe = \left| \overrightarrow{v_{e,h}} \right| L / D_{e,h} = \mu_{e,h} \left| \vec{E} \right| L / D_{e,h} = \left| \vec{E} \right| L / U_T \quad (2)$$

With L the characteristic transport length, E the electric field, U_T the thermodynamic potential, $v_{e,h}$, $\mu_{e,h}$ and $D_{e,h}$ the velocity, mobility and diffusion coefficient of electrons and holes, respectively.

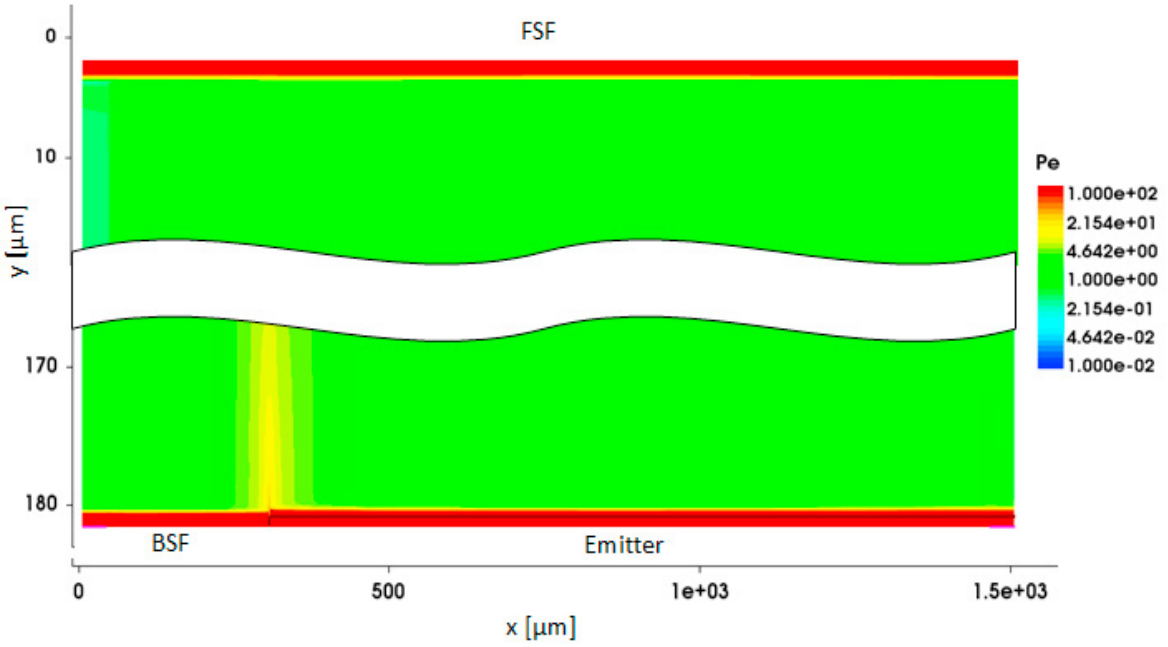

Fig. 2. Peclet number of an IBC cell with α=0.8 at mpp

We first observe that the Peclet number is the same for electrons and holes, making this criterion suitable for the description of the nature of the transport of a bipolar current. The characteristic transport length is defined in hydrology as the typical length over which the transport occurs. In our case we will use the distance between two electrodes of opposite polarity.

We can then observe in Fig. 2 that all heavily doped layers of an IBC solar cell show a Pe above 100 indicating the clear dominance of drift as main transport mechanism. As additionally the main carrier type contributing to the current in these regions are the majority carriers, one can state that the majority carrier Joule losses obtained by the FELA is a very good approximation of the Joule losses induced by a series resistance.

On the contrary, the bulk shows in average a value of Pe close to 1 indicating that drift and diffusion play a comparable role in carrier transport. While the equivalence of Joule losses made for heavily doped regions may not be made for the bulk, we will show in the following of this article that in practice it is a quite good approximation while accuracy, however, reduces toward high injection.

Making the equivalence between the power dissipated by the solar cell element and by a resistance crossed by the same current at mpp, the series resistance $R_{s,i}$ of this element i can then be extracted as

$$R_{s,i} = \Phi_{maj,i} / J_{mpp}^{\ 2} \tag{3}$$

2.3. R_s of studied IBC solar cell

We simulated the IBC solar cell described in Sec. 2.1 with TCAD Sentaurus where the two investigated bulk resistivities (1 and 8 Ωcm) bring the bulk in relatively low injection ($\Delta n \approx N_D/5$) and moderately to high injection ($\Delta n \approx 2\text{-}5*N_D$), respectively, at mpp.

When the IBC solar cell uses an FSF, it has to be considered in parallel to the bulk and only the parallel arrangement of the bulk and the FSF should be considered as a component of series resistance. However, to bring information about the influence of the FSF on the series resistance, we will show its contribution to the R_s.

The R_s of each solar cell part is extracted from TCAD simulation using Eq. 3 and the sum of all contributions is compared to the lumped R_s extracted using the multiple light intensity method (MLIM) [13,14]. Compared to other methods to extract R_s, the MLIM has the advantage not to presume the characteristics of the diode network used in the equivalent circuit modeling of the solar cell, requiring only that the network properties do not depend on illumination.

On all graphs of Fig. 3 we observe that the series resistance of the BSF and the emitter do not vary linearly with α as it would be predicted by analytical formulae [1]. This is because the derivation of this formula assumed a homogeneous current density at the BSF / emitter interface with the bulk which is not correct as one can see in Fig. 4. As mentioned in the last section, the extraction of the series resistance of the heavily doped part by this method is accurate and therefore, as the TCAD simulates correctly the current distribution, this method allows taking these non-linear phenomena into account in the series resistance analysis, leading to a more realistic description of the solar cell.

We then observe in Fig. 3 (c) and (d) that the series resistance of the solar cell with low bulk resistivity is well estimated by this method for all α. Therefore, despite the fact that drift and diffusion contribute equally to the carrier transport in the bulk, the estimation of its series resistance through the majority carrier Joule losses is a good approximation in low injection condition.

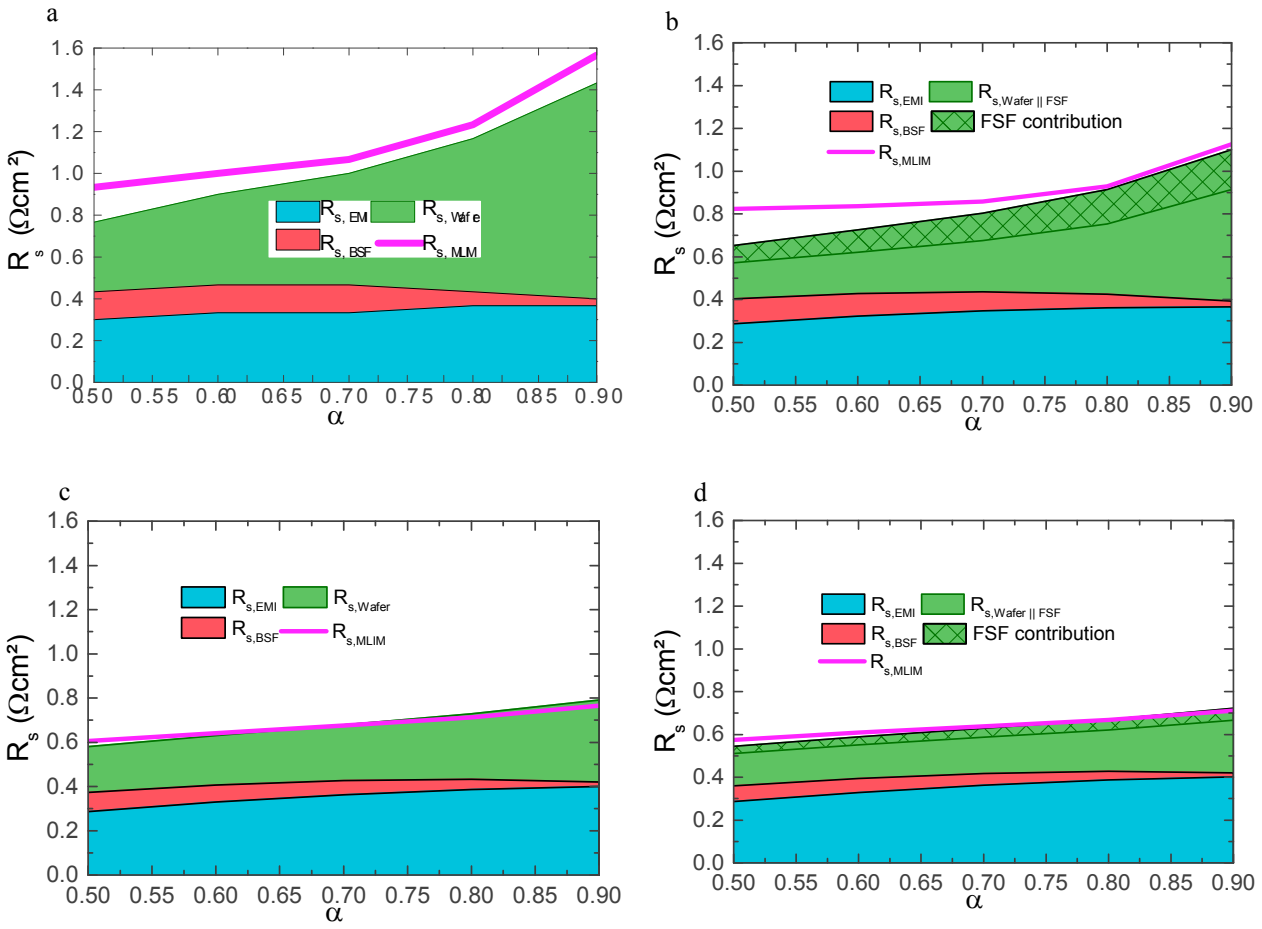

Fig. 3. R_s extracted for various parts of a typical IBC solar cell with varying emitter fraction with ((b) and (d)) and without an FSF ((a) and (c)) with a 1 Ωcm ((c) and (d)) and 8 Ωcm ((a) and (b)) bulk resistivity compared to the lumped R_s from MLIM (pink line).

However, we see in Fig. 3 (a) and (b) that the FELA slightly underestimates the series resistance for a solar cell with high bulk resistivity and low α. In general cells with low α have a very high density of minority carriers in the bulk above the emitter (with reference to N_d = 6e14 cm^{-3}) that puts this part of the bulk in high injection (see Fig. 4). The non negligible current crossing this area is therefore composed of as much electrons as holes. In this region, considering only the Joule losses of the electrons for the calculation of R_s leads therefore to its underestimation. We cannot, however, simply add the Joule losses of the minority carriers since a large part of it is associated with transport towards an area of recombination or collection by diffusion [15].

One should additionally mention that the validity of the MLIM in this case may be doubted. Indeed, in high injection, the injection is not only a function of the cell bias but also of illumination. As the recombination properties of the cell and thus their description by a diode network in an equivalent circuit depend explicitly on the injection, one could state that the diode network properties become a function of illumination which is an explicit violation of the only assumption used for MLIM exploitation. On the other hand the MLIM extraction of R_s using 3 different illumination levels allowed to cross check the linearity of the defining relation of the MLIM ($\Delta V=R_s . \Delta J_{sc}$ see [6]) which is excellent (R=0.9999) and only very slightly worse for high injection cases (R=0.9995). It is therefore not clear how strong this violation of the assumption of the MLIM hinders its validity in high injection cases. The MLIM remains in our opinion the method that gives the most reliable value of R_s from the experimental

point of view, though this value remains an approximation and does not constitute, strictly speaking, an absolute definition of R_s.

In case where the cell has a high α, a significant discrepancy between series resistance determined by FELA and that from MLIM occurs only for the cell without an FSF (Fig. 3 (a)). As the injection in the bulk is comparable with or without an FSF, and much smaller than the injection for cells with low α (Fig. 4), the injection does not explain alone the observed discrepancy. However, without an FSF, there is a much bigger zone of high current density which is extending towards the front surface. One observes also in Fig. 3 (a) that the contribution of the bulk in this case is almost 1 Ωcm^2 and thus incompleteness in the description of the series resistance can lead to a larger discrepancy between the MLIM and the FELA value of R_s.

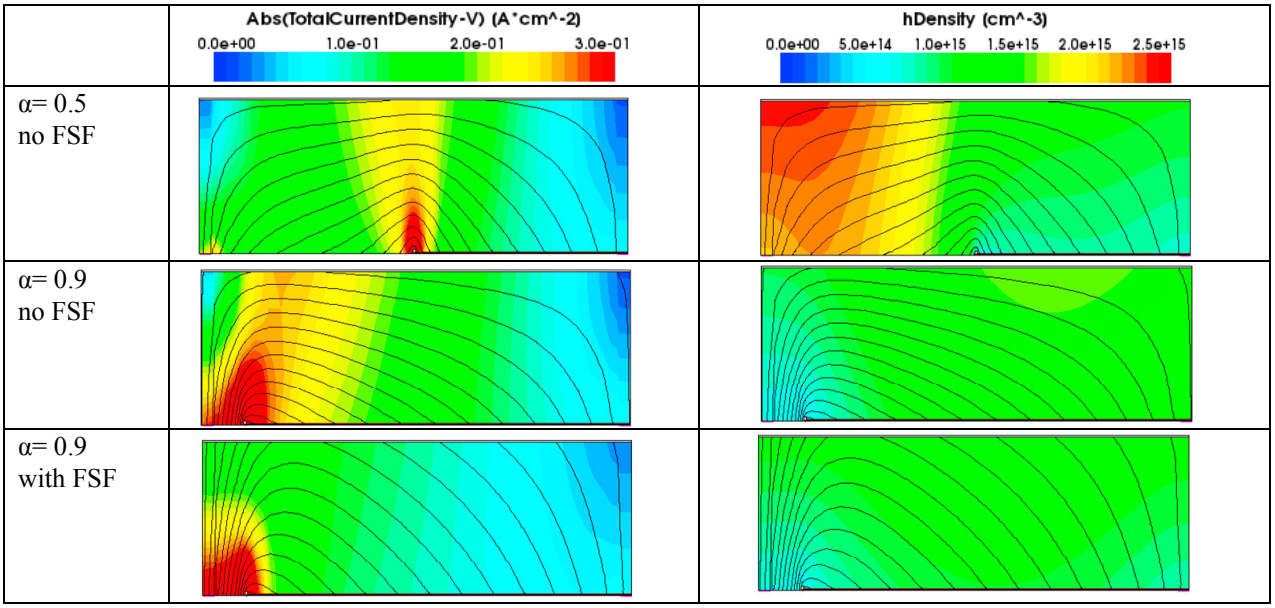

Fig. 4. Total current density (left) and hole density (minority carriers, right) distribution for various cells studied in Fig. 3. The contour lines represent the total current flow lines.

The overall error of this method is relatively low for all investigated cases and also of the order of a measurement error when applying the MLIM to a real solar cell. This method allows therefore a reliable estimation of individual components of series resistance from a TCAD simulation.

3. Summary and outlook

We introduced a method for computing the individual components of the series resistance of a solar cell out of a bipolar TCAD simulation. This method is based on the identification of the Joule losses of the majority carriers obtained by the FELA to the Joule losses dissipated by the series resistance. We justified this approach for highly doped areas by showing that drift is the dominant transport mechanism using a criterion based on the Peclet number and that minority carriers play a minor role in the current density as their density is very low.

While such argument does not apply to the bulk, we showed that the result of the method remains accurate providing the bulk is in low injection.

In case of high injection, the method underestimates the series resistance presumably because a part of the minority carriers contributes to the electrical current transport additionally to the majority carriers. This part can, however, not be estimated accurately as most of the minority carrier current is associated to transport toward recombination regions by diffusion. The underestimation is, however, reasonable and of the order of a typical measurement error.

With such a decomposition of the individual components of the series resistance out of a simulation it is possible to optimize each part of new solar cell architectures where 2- or 3-dimensional carrier flows occur with respect to series resistance and cross check with MLIM measurements.

Acknowledgements

Part of this work was supported by the German Federal Ministry for Economic Affairs and Energy under contract number FKZ 0324001.

References

[1] Yang Y, Xu G, Zhang K, Zhang X, Shen H, Altermatt PP, Verlinden P, Feng Z. Analysis of series resistance of industrial crystalline silicon solar cells by numerical simulations and analytical modeling. Proc. 28th EUPVSEC, Paris 2013, p. 1558-61.
[2] Verlinden PJ, Aleman M, Posthuma N, Fernandez J, Pawlak B, Robbelein J, Debucquoy M, Van Wichelen K, Poortmans J. Simple power-loss analysis method for high-efficiency Interdigitated Back Contact (IBC) silicon solar cells. Sol En Mat & Sol Cells 2012;106:37-41.
[3] Kluska S, Granek F, Rüdiger M, Hermle M, Glunz SW. Modeling and optimization study of industrial n-type high-efficiency back-contact back-junction silicon solar cells. Sol En Mat & Sol Cells 2010;94;568-77.
[4] Eidelloth S, Haase F, Brendel R. Simulation tool for equivalent circuit modeling of photovoltaic devices. IEEE J Photovolt 2012;2:572-9.
[5] Mackel H, Micard G, Varner K. Analytical models for the series resistance of selective emitters in silicon solar cells including the effect of busbars. Prog Photovolt 2015;23:135-49.
[6] Micard G, Hahn G. Discussion and simulation about the evaluation of the emitter series resistance. Proc. 28th EUPVSEC, Paris 2013, p. 815-21.
[7] Gurevich Y. Lashkevych I. Sources of fluxes of energy, heat, and diffusion heat in a bipolar semiconductor: Influence of nonequilibrium charge carriers. Int J Thermophysics 2013;34:341-9.
[8] Smith D, Cousins P, Westerberg S, De Jesus-Tabajonda R, Aniero G, Shen Y-C. Toward the practical limits of silicon solar cells. IEEE J Photovolt 2014;4:1465-9.
[9] Brendel R, Dreissigacker S, Harder N-P, Altermatt PP. Theory of analyzing free energy losses in solar cells, Appl Phys Lett 2008;93:173503.
[10] Altermatt PP. Models for numerical device simulations of crystalline silicon solar cells-a review. J Comput Electron 2011:10:314-30.
[11] Franklin E, Fong K, McIntosh K,Fell A, Blakers A, Kho T, Walter D, Wang D, Zin N, Stocks M, Wang E-C, Grant N, Wan Y, Yang Y, Zhang X, Feng Z, Verlinden P. Fabrication and characterization of a 24.4% efficient IBC cell. Proc. 29th EUPVSEC, Amsterdam 2014, p. 666-71.
[12] Rao Govindaraju S, Bhabani Das S. Moment analysis for subsurface hydrologic applications. Springer 2007
[13] Wolf M, Rauschenbach H. Series resistance effects on solar cell measurements. Adv Energy Convers 1963;3:455-79.
[14] Fong KC, McIntosh KR, Blakers AW. Accurate series resistance measurement of solar cells. Prog Photovolt 2013;21:490-9.
[15] Micard G, Hahn G. Free energy loss analysis decomposition of the power voltage characteristic of an interdigitated back contact solar cell. Proc. 29th EUPVSEC, Amsterdam 2014, p. 1267-71.